

# Relative clinical utility of simultaneous $^{18}\text{F}$ -fluorodeoxyglucose PET/MRI and PET/CT for preoperative cervical cancer diagnosis

Jing Gong<sup>1,\*</sup> , Honghong Liu<sup>2,\*</sup>,  
Zhaoliang Bao<sup>1</sup>, Lihua Bian<sup>3</sup>, Xiuzhen Li<sup>4</sup> and  
Yuanguang Meng<sup>3</sup>

## Abstract

**Objective:** To investigate the utility of  $^{18}\text{F}$ -fluorodeoxyglucose ( $^{18}\text{F}$ -FDG) positron emission tomography/magnetic resonance imaging (PET/MRI) for the preoperative diagnosis of cervical cancer.

**Methods:** We retrospectively analyzed 114 patients who were diagnosed with cervical cancer and underwent PET/MRI ( $n = 59$ ) or PET/computed tomography (PET/CT) ( $n = 65$ ) before surgery. The maximal standardized uptake value ( $\text{SUV}_{\text{max}}$ ) and mean SUV ( $\text{SUV}_{\text{mean}}$ ) were determined for regions of interest in the resultant radiographic images.

**Results:** Relative to PET/CT,  $^{18}\text{F}$ -FDG PET/MRI exhibited higher specificity and sensitivity in defining the primary tumor bounds and higher sensitivity for detection of bladder involvement. The  $\text{SUV}_{\text{max}}$  and  $\text{SUV}_{\text{mean}}$  of PET/MRI were remarkably higher than those of PET/CT as a means of detecting primary tumors, bladder involvement, and the lymph node status. However, no significant differences in these values were detected when comparing the two imaging approaches as a means of detecting vaginal involvement or para-aortic lymph node metastasis.

<sup>4</sup>Department of Obstetrics and Gynecology, People's Hospital of Shuangluan District, Chengde City, Hebei Province, China

\*These authors contributed equally to this work.

### Corresponding author:

Yuanguang Meng, Department of Obstetrics and Gynecology, The First Medical Center of Chinese PLA General Hospital, No. 28 Fuxing Road, Beijing 100853, China.

Email: jingg2020\_@163.com

<sup>1</sup>Department of Obstetrics and Gynecology, Beijing Anzhen Hospital, Capital Medical University, Beijing, China

<sup>2</sup>Department of Nuclear Medicine, The First Medical Center of Chinese PLA General Hospital, Beijing, China

<sup>3</sup>Department of Obstetrics and Gynecology, The First Medical Center of Chinese PLA General Hospital, Beijing, China



**Conclusions:** These outcomes may demonstrate the capability of  $^{18}\text{F}$ -FDG PET/MRI to clarify preoperative cervical cancer diagnoses in the context of unclear PET/CT findings. However, studies directly comparing SUVs in different lesion types from patients who have undergone both PET/MRI and PET/CT scans are essential to validate and expand upon these findings.

### Keywords

$^{18}\text{F}$ -fluorodeoxyglucose positron emission tomography/magnetic resonance imaging, positron emission tomography/computed tomography, cervical cancer, preoperative diagnosis, clinical application, standardized uptake value

Date received: 24 January 2021; accepted: 26 April 2021

### Introduction

Cervical cancer is among the most common malignancies in women, with more than 50 million newly reported cases and 27 million cervical cancer-related deaths occurring worldwide each year.<sup>1</sup> When restricted to the lower pelvis, cervical cancer is generally curable through chemoradiotherapy and/or surgery.<sup>2</sup> Several preoperative prognostic factors, including the clinical stage, diameter, and volume of the tumor, are helpful for prediction of the prognosis in patients with cervical cancer.<sup>3–5</sup> However, traditional imaging modalities are limited in their ability to measure such prognostic parameters. In comparison with surgical staging, clinical staging based on the criteria of the International Federation of Gynecology and Obstetrics (FIGO) can insufficiently stage as many as 30% of patients with stage IB and 64% of patients with stage IIIB cervical cancer.<sup>6</sup> The use of more advanced imaging approaches, including magnetic resonance imaging (MRI), computed tomography (CT), and fluorine-18-labeled fluorodeoxyglucose positron emission tomography ( $^{18}\text{F}$ -FDG PET), can improve clinicians' ability to accurately diagnose and treat cervical cancer.<sup>7,8</sup>

Since their advent, PET/CT imaging technologies have continued to advance,

leading to major improvements in image quality.<sup>9,10</sup> Although combination PET/CT imaging has been highly successful, researchers have explored its replacement with combination PET/MRI<sup>11,12</sup> because MRI scans provide higher resolution, reduce patient radiation exposure, and expand functional and molecular imaging options relative to CT. MRI scans cannot readily replace CT components in existing PET/CT scanners; however, technical modifications of MRI and PET instruments are required to obtain fully integrated PET/MRI scans. MRI and PET can also interfere with one another through field gradients or MR radiofrequency.<sup>13,14</sup> However, PET/MRI may be a valuable technique for patients with endometrial and cervical cancer.<sup>15</sup> It is also essential that accurate MRI-based approaches be used for PET emission data attenuation correction, specifically for quantitative PET. Whereas CT scans measure tissue attenuation coefficients in response to X-ray exposure, MRI signals are impacted by hydrogen density and relaxation within target tissues,<sup>16,17</sup> making 511-keV photon attenuation coefficient derivation more challenging for MRI than for CT. Many researchers to date have highlighted the clinical feasibility of whole-body

PET/MRI scans in patients with various types of cancers by comparing these scan results to those derived from PET/CT scanning.<sup>18–21</sup> Such whole-body PET/MRI scans can yield high-quality images that are associated with small but significant differences in tracer dosage.

In the present study, we compared the outcomes of whole-body <sup>18</sup>F-FDG PET/MRI and PET/CT in an effort to understand the potential of <sup>18</sup>F-FDG PET/MRI for the preoperative evaluation of patients with cervical cancer and to summarize the clinical significance of quantitative indicators associated with this imaging approach.

## Materials and methods

### Patients

This study was approved by the ethics committee of Beijing Anzhen Hospital (approval no.: 2019079X). The ethics board in the hospitals waived the requirement for obtaining informed consent from the patients because this was a retrospective investigation. However, we obtained patient consent for treatment, and all patient details have been de-identified. This study involved 124 patients who received a histological diagnosis of primary cervical cancer and underwent PET/MRI or PET/CT from January 2013 to December 2017 in the Obstetrics and Gynecology Department of Chinese PLA General Hospital. For this study, we selected patients who had cervical cancer that had been positively diagnosed via biopsy, had undergone preoperative PET/MRI or PET/CT evaluation, underwent radical or modified radical hysterectomy, had complete case data, and provided written informed consent.

We excluded patients who were claustrophobic, were unable to satisfactorily control their breathing, declined to undergo PET/MRI or PET/CT imaging, were allergic to

the <sup>18</sup>F-FDG contrast agent, had coagulation disorders, had other concomitant tumors, had other serious medical conditions, or were unable to tolerate anesthesia or surgery. Fifty-nine patients underwent whole-body <sup>18</sup>F-FDG PET/MRI scanning and 65 patients underwent <sup>18</sup>F-FDG PET/CT scanning; these latter 65 patients served as the control group in the present analysis. Cancer staging was conducted based on the FIGO cancer staging system. Patients with stage IA, IB1, IIA1, and IIA2 disease were treated via modified radical hysterectomy, while those with stage IB2 and IIB disease were treated via radical hysterectomy. The overall demographic information of the patients in the present study is shown in Table 1.

### <sup>18</sup>F-FDG PET/CT

All patients fasted for a minimum of 6 hours before <sup>18</sup>F-FDG PET/CT imaging. The scan was then performed with a 64-row multidetector PET/CT system (Biograph<sup>TM</sup> TruePoint<sup>TM</sup> 64; Siemens AG, Munich, Germany) equipped for a four-ring PET scanner and a 40-section CT scanner. PET images were collected following intravenous administration of <sup>18</sup>F-FDG (555 MBq) for 50 to 70 minutes from the vertex to mid-thigh, and a 1.5-minute scan time per table position was used (matrix size, 512 × 512). This PET scanner had a spatial resolution of 4.4-mm full width at half maximum (FWHM) at 1 cm and 5.2-mm FWHM at 10 cm from the transverse field of view (FOV), with a sensitivity of 9.7 kcps/MBq at the center of the FOV. Prior to PET acquisition, a standard helical low-dose CT scan (120 kV, 80 mA, 0.8 s/rotation, pitch 1.5, 3.75-mm slice thickness) was acquired from the head to the proximal thigh using the CARE kV and CARE Dose 4D dose reduction software provided by the manufacturer. Intravenous iodinated contrast was not

**Table 1.** Patient demographics.

Demographics	PET/MRI group	PET/CT group	$t/\chi^2$	$p$ -value*
Number of patients	59	65		
Age, years	58.9 ± 6.2	57.7 ± 7.3	0.981	0.328
BMI, kg/m <sup>2</sup>	23.2 ± 2.4	22.6 ± 2.5	1.360	0.176
Previous abdominal surgery	12 (20.3)	15 (23.1)	0.136	0.712
Hysterectomy			1.268	0.260
Modified radical (type B)	35 (59.3)	32 (49.2)		
Radical (type C)	24 (40.7)	33 (50.8)		
FIGO stage			5.901	0.316
IA	13 (22.0)	14 (21.6)		
IB1	21 (35.6)	16 (24.6)		
IB2	3 (5.1)	7 (10.8)		
IIA1	7 (11.9)	16 (24.6)		
IIA2	4 (6.8)	3 (4.6)		
IIB	11 (18.6)	9 (13.8)		

Data are presented as mean ± standard deviation or n (%).

\* $p > 0.05$  was not considered statistically significant.

PET: positron emission tomography, MRI: magnetic resonance imaging, CT: computed tomography, BMI: body mass index, FIGO: International Federation of Gynecology and Obstetrics.

administered to any patients. Following scanning, PET image reconstruction and CT attenuation correction were completed through the use of an ordered-subset expectation maximization iterative reconstruction algorithm (2 iterations and 21 subsets).

### <sup>18</sup>F-FDG PET/MRI

<sup>18</sup>F-FDG PET/MRI scans were conducted in 59 patients using a Magnetom Biograph mMR instrument (Siemens Healthineers, Erlangen, Germany) equipped with a strength of the 3T magnetic field, whole-body imaging matrix coil technology with radiofrequency surface coils having multiple integrations, and a PET system of fully functional condition with embedded avalanche photodiode technology in the MR gantry. Three hybrid PET/MRI platforms have been marketed to date: simultaneous PET/MRI, sequential PET/MRI, and sequential PET/CT-MRI<sup>22</sup>; the instrument used in this study was a simultaneous

PET/MRI instrument. All patients fasted for 6 hours prior to scanning, after which they were intravenously administered a body weight-appropriate dose of <sup>18</sup>F-FDG (4 MBq/kg; mean, 285 ± 70 MBq; range, 154–456 MBq). Following a 2-hour period of <sup>18</sup>F-FDG administration, PET/MRI was initiated.

The PET scanner had a 4.4-mm FWHM spatial resolution at 1 cm, with a resolution of 5.3-mm FWHM at 10 cm from the transverse FOV. We conducted the whole-body PET scanning in four bed positions from the vertex to the mid-thigh, with an acquisition time of 5 minutes per position. Simultaneous whole-body MRI scanning was also conducted in the same positions with a sagittal short tau inversion recovery (STIR) sequence and a breath-holding half-Fourier single-shot turbo spin echo (HASTE) sequence. Regional PET was conducted with a 10-minute acquisition time. Pelvic MRI was conducted using previously reported sequences<sup>23</sup> as follows

**Table 2.** Comparison of diagnostic indicators between imaging detection technology and surgical pathology.

	PET/MRI group	PET/CT group	$t/\chi^2$	p-value
<b>Primary lesions</b>				
<2 cm, Sens (n)	94.4% (17/18)	61.9% (13/21)	5.781	0.016*
2–4 cm, Sens (n)	89.7% (26/29)	68.6% (24/35)	4.125	0.042*
>4 cm, Sens (n)	100% (12/12)	66.7% (6/9)	4.667	0.031*
<b>Vaginal involvement</b>				
Sens (n)	100% (11/11)	78.9% (15/19)	2.672	0.102
Spec (n)	97.9% (47/48)	93.5% (43/46)	1.136	0.287
<b>Bladder involvement</b>				
Sens (n)	80.0% (4/5)	14.3% (1/7)	5.182	0.023*
Spec (n)	90.7% (49/54)	96.6% (56/58)	1.612	0.204
<b>Pelvic lymph node metastasis</b>				
Sens (n)	96.2% (25/26)	93.1% (27/29)	0.247	0.619
Spec (n)	87.9% (29/33)	91.7% (33/36)	0.271	0.603
<b>Para-aortic lymph node metastasis</b>				
Sens (n)	100% (4/4)	33.3% (2/6)	4.444	0.035*
Spec (n)	83.6% (46/55)	74.6% (44/59)	1.406	0.236

\* $p < 0.05$  was considered statistically significant.

PET: positron emission tomography, MRI: magnetic resonance imaging, CT: computed tomography, Sens: diagnostic sensitivity, Spec: diagnostic specificity.

(Table 2): a transverse T2 turbo spin echo (TSE) sequence, a sagittal T2 TSE sequence, a transverse T1 TSE sequence, a transverse fat-saturated T1 TSE following intravenous contrast administration (0.1 mmol/kg gadobutrol (Gadavist; Bayer Healthcare, Germany)), a sagittal post-contrast T1 TSE, and a transverse diffusion-weighted echo-planar imaging sequence using two b-values: b0 and b1000 s/mm<sup>2</sup>. Following scan completion, an ordinary Poisson ordered-subset expectation maximization approach (3 iterations, 21 subsets, a 4-mm Gaussian post-processing filter, and matrix size of 512 × 512) was used for image reconstruction.

### Image analyses and reference standards

Fellowship-trained nuclear medicine physicians and radiologists respectively analyzed the PET/MRI and PET/CT images with a dedicated program (syngo.via; Siemens

Healthineers). Focal lesions in PET images exhibiting enhanced glucose uptake in comparison to surrounding tissue were deemed suspicious. To effectively identify every region of possible microscopic disease, all submucosal abnormalities in MRI were presumed to be associated with tumor infiltration consistent with current clinical standards aimed at encompassing all abnormal parts within the imaged field.<sup>24</sup> Regional lymph nodes were deemed metastatic when extracapsular spread or necrosis was detected or when a cluster of borderline size 3+ lymph nodes was detected. The diagnosis of distant metastases was based upon morphological lesion and contrast enhancement patterns.

When assessing the scan results, the reviewers were requested to evaluate both technical feasibility and diagnostic performance parameters, rating the overall PET image quality for PET/CT and PET/MRI scans as follows: 1 = nondiagnostic, 2 = poor, 3 = good, and 4 = excellent.

The maximal standardized uptake value ( $SUV_{max}$ ) and mean SUV ( $SUV_{mean}$ ) for primary tumors, metastases, and metastatic lymph nodes were used as a means for quantitative analysis of the diagnostic efficacy of the PET/MRI scans. For these analyses, a volume of interest surrounding these lesions was drawn with the isocontour function of the volume of interest in the analytical software with a  $SUV_{max}$  threshold of 40%.

We analyzed the identified primary cervical cancers via the cognitive fusion of diffusion-weighted images and T2-weighted images. The scanning software generated apparent diffusion coefficient (ADC) maps in an automated manner. Tumor diffusion parameters were calculated by manually marking tumor tissue borders using a polygonal region of interest in each ADC map slice.

### **Statistical analysis**

The relative sensitivity and specificity for each imaging modality were calculated. Data analyses and figure construction were conducted using OriginPro 2016 (OriginLab Corporation, Northampton, MA, USA) and SPSS for Windows, Version 16.0 (SPSS Inc., Chicago, IL, USA). Quantitative data are given as mean  $\pm$  standard deviation and were compared via one-way analysis of variance and Student's t-test. Confidence thresholds for these analyses were set at 95% and 99%.

## **Results**

### **Patient characteristics**

This study involved 124 patients with untreated histologically confirmed primary cervical cancer from January 2013 to December 2017. Of these patients, whole-body  $^{18}F$ -FDG PET/MRI scanning was performed for 59 patients, while 65 underwent  $^{18}F$ -FDG PET/CT scanning.

As shown in Table 1, no significant differences in the patients' age, body mass index, surgical strategy, FIGO cancer stage, or history of abdominal surgery were found between the PET/CT and PET/MRI groups, enabling comparative analyses between these two patient groups.

### **Comparison of diagnostic indicators between imaging detection technology and surgical pathological findings using histopathology as gold diagnostic standard**

Excellent-quality images (score of 4) were obtained for all scans (PET/CT and PET/MRI) recorded in this study, with representative images shown in Figures 1 and 2, respectively. No detectable errors were observed in any MR attenuation correction map reads, and perfect spatial coregistration ( $<2$ -mm mismatch) was observed between PET and MRI or CT in all patients. Relative to PET/CT, higher sensitivity and specificity were observed for  $^{18}F$ -FDG PET/MRI when defining the primary tumor extent (Figures 1d and 2d, red arrow). After undergoing PET/CT or PET/MRI, all patients underwent modified radical or radical hysterectomy as appropriate, and all tumor tissues were then subjected to immediate pathological analysis (data not shown). Comparisons of the diagnostic indicators associated with these two imaging approaches and surgical pathology are shown in Table 2. When assessing primary tumors,  $^{18}F$ -FDG PET/MRI showed significantly higher sensitivity than PET/CT (94.4% vs. 61.9% for  $<2$ -cm primary lesions,  $p=0.016$ ; 89.7% vs. 68.6% for 2- to 4-cm primary lesions,  $p=0.042$ ; and 100% vs. 66.7% for  $>4$ -cm primary lesions,  $p=0.031$ ).

As a means of assessing vaginal involvement, however, the differences in diagnostic sensitivity and specificity were not

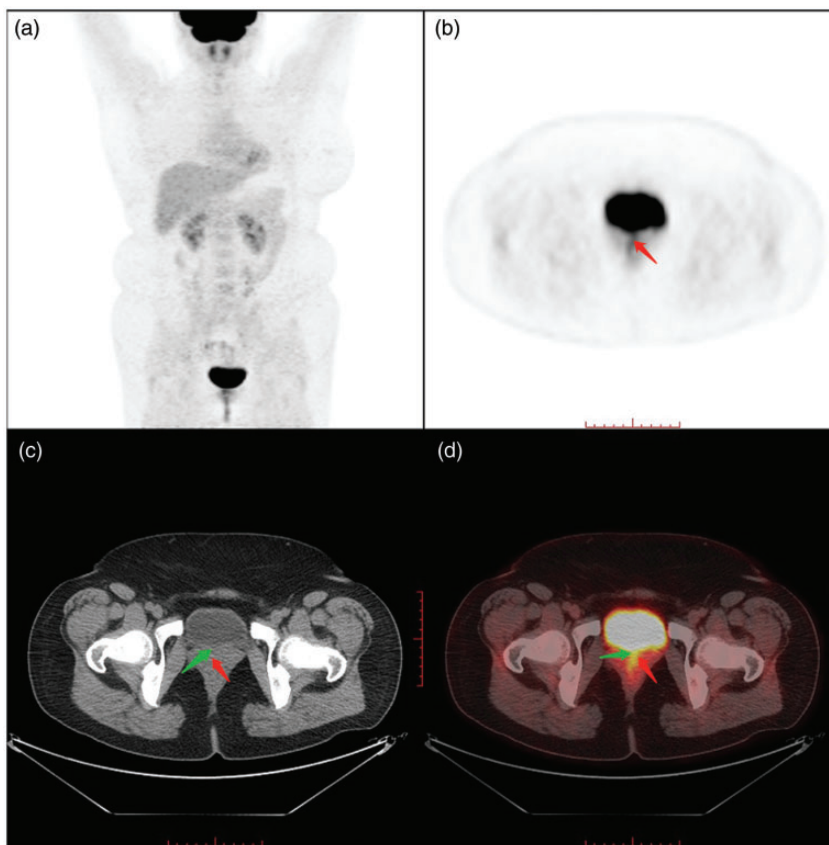


**Figure 1.** Imaging findings in a 26-year-old patient with FIGO IBI cervical cancer. (a) Whole-body  $^{18}\text{F}$ -FDG uptake. (b) Tumor and uterine cervix  $^{18}\text{F}$ -FDG uptake map. (c) Tumor CT map. (d) Fused  $^{18}\text{F}$ -FDG PET/CT image of tumor lesion map.

statistically significant between PET/MRI and PET/CT. In contrast, these two approaches exhibited significant differences in diagnostic sensitivity when used to assess bladder involvement ( $p = 0.023$ ). Similarly, for detecting pelvic lymph node metastasis via  $^{18}\text{F}$ -FDG PET/MRI and  $^{18}\text{F}$ -FDG PET/CT on a per-level basis, the specificity and sensitivity were 96.2% vs. 93.1% and 87.9% vs. 91.7%, respectively, with no significant differences. However, PET/MRI showed significantly higher sensitivity than PET/CT when used to detect para-aortic lymph node metastases (100% vs. 33.3%,  $p = 0.035$ ).

### Quantitative lesion analysis

During the analysis of only primary tumors, both the  $\text{SUV}_{\text{mean}}$  and  $\text{SUV}_{\text{max}}$  were significantly higher in the PET/MRI group than in the PET/CT group ( $p < 0.001$ ) (Table 3). The  $\text{SUV}_{\text{max}}$  and  $\text{SUV}_{\text{mean}}$  differed by 57% and 54%, respectively, between PET/MRI and PET/CT. When specifically assessing vaginal involvement, however, no significant difference was observed in the  $\text{SUV}_{\text{max}}$  or  $\text{SUV}_{\text{mean}}$  of these two groups (Table 3). In contrast, when evaluating bladder involvement, the  $\text{SUV}_{\text{max}}$  and  $\text{SUV}_{\text{mean}}$  were significantly

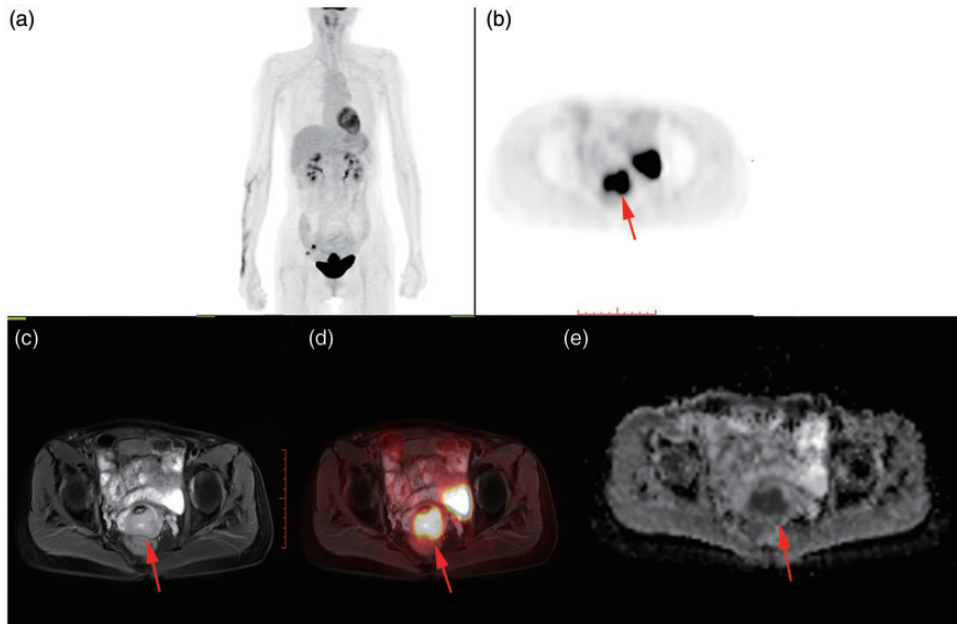


**Figure 2.** Imaging findings in a 56-year-old patient with FIGO IBI cervical cancer. (a) Whole-body  $^{18}\text{F}$ -FDG uptake. (b) Uterine cervix  $^{18}\text{F}$ -FDG uptake. (c) T2-weighted MRI. (d) Fused  $^{18}\text{F}$ -FDG PET/T2-weighted MRI of the lesion. (e) Tumor ADC map.

higher in the PET/MRI group than in the PET/CT group ( $p < 0.001$ ) (Table 3). Finally, when analyzing para-aortic lymph node metastases, the  $\text{SUV}_{\text{max}}$  and  $\text{SUV}_{\text{mean}}$  were also significantly higher in the PET/MRI group than in the PET/CT group ( $p < 0.001$ ). No significant differences were found for pelvic lymph node metastases (Table 3).

## Discussion

PET/CT and PET/MRI are multimodal imaging strategies that have seen increasing clinical use in recent years.<sup>25</sup> PET scanning allows researchers and radiographers to gain tissue metabolism-based insights by analyzing tissues labeled with the  $^{18}\text{F}$ -FDG positron emission nuclide.<sup>26</sup> In contrast, MRI and CT scans offer detailed anatomical information pertaining to human bone and soft tissue structures.<sup>27,28</sup>

By integrating PET scans with CT or MRI data, clinicians can obtain whole-body images of the  $^{18}\text{F}$ -FDG metabolism profiles of patients with cancer. Rapid tumor cell proliferation and associated increases in glucose uptake and utilization allow for early-stage malignancies to be detected in an extremely sensitive manner via this approach. Because of the high sensitivity to intratumoral metabolic changes using this approach, it is possible to identify the tumor size, scope, degree of malignancy, and TNM staging.<sup>29</sup>

Several studies to date have analyzed the PET/CT applications for evaluating gynecological tumors. Bollineni et al.<sup>30</sup> performed a meta-analysis on this topic and found that PET/CT was able to achieve specificity and sensitivity of 90.4% and 82.8%, respectively, for lymph node metastasis in patients with cervical cancer and other gynecological malignancies. While PET/MRI-related



**Table 3.** Quantitative evaluation of lesions.

	PET/MRI group	PET/CT group	$t/\chi^2$	$p$ -value
<b>Primary lesions</b>				
SUV <sub>max</sub>	23.7 ± 8.1 (59)	15.1 ± 5.6 (65)	8.364	<0.001*
SUV <sub>mean</sub>	14.2 ± 4.6 (59)	9.2 ± 4.8 (65)	9.256	<0.001*
<b>Vaginal involvement</b>				
SUV <sub>max</sub>	14.5 ± 7.7 (58)	13.7 ± 5.9 (58)	0.164	0.311
SUV <sub>mean</sub>	8.0 ± 4.3 (58)	9.4 ± 6.8 (58)	0.178	0.308
<b>Bladder involvement</b>				
SUV <sub>max</sub>	17.6 ± 8.2 (53)	12.3 ± 3.5 (57)	5.182	<0.001*
SUV <sub>mean</sub>	10.5 ± 5.6 (53)	5.6 ± 4.4 (57)	1.612	<0.001*
<b>Pelvic lymph node metastasis</b>				
SUV <sub>max</sub>	16.4 ± 5.8 (54)	15.9 ± 6.9 (60)	0.127	0.413
SUV <sub>mean</sub>	10.2 ± 7.3 (54)	9.3 ± 5.2 (60)	0.103	0.525
<b>Para-aortic lymph node metastasis</b>				
SUV <sub>max</sub>	13.6 ± 9.3 (50)	6.3 ± 7.9 (46)	6.256	<0.001*
SUV <sub>mean</sub>	9.5 ± 6.2 (50)	4.3 ± 2.8 (46)	8.118	<0.001*

Data are presented as mean ± standard deviation (n).

\*  $p < 0.05$  was considered statistically significant.

PET: positron emission tomography, MRI: magnetic resonance imaging, CT: computed tomography, SUV<sub>max</sub>: maximal standardized uptake value, SUV<sub>mean</sub>: mean standardized uptake value.

evidence-based medicines are still in their infancy, this combined imaging modality offers various advantages over more traditional imaging conducted by PET/CT. First, MRI offers better soft tissue imaging quality than does CT, making it better suited to the evaluation of specific tissues and organs through functional imaging approaches that are incompatible with CT.<sup>31</sup> In the present analysis, the diagnostic sensitivity was significantly higher in the PET/MRI group than in the PET/CT group for primary lesions of <2 cm (94.4% vs. 61.9%), 2 to 4 cm (89.7% vs. 68.6%), and >4 cm (100.0% vs. 66.7%) ( $p < 0.05$ ). This suggests that PET/MRI scans are better suited to evaluating the lesion scope, providing radiographers and clinicians with additional insight into the tumor stage and status that can guide surgical and treatment planning.

Second, PET/MRI combination imaging can overcome the limitations of sequential PET/CT imaging by enabling complete synchronization of PET and MRI image acquisition, thus permitting simultaneous

anatomical and functional metabolic analyses. In this study, a significantly higher diagnostic sensitivity was observed for PET/MRI than for PET/CT when evaluating para-aortic lymph node metastasis (100.0% vs. 33.3%,  $p < 0.05$ ). This finding is clinically significant in the context of lymphadenectomy and pelvic external beam radiotherapy implementation in patients with cervical cancer patients. Kim et al.<sup>32</sup> observed that <sup>18</sup>F-FDG PET/MRI scans offered 100% sensitivity and 96% specificity when used to detect early cervical cancer lymph node metastases of >5 mm in diameter, which was superior to PET/CT and in line with our findings. Third, PET/MRI scans can markedly reduce patient radiation exposure to roughly 20% of that associated with PET/CT scans.<sup>33</sup>

Efforts to quantify PET/MRI- and PET/CT-based tumor diagnostic modalities to date have been largely focused on indicators including the SUV, ADC, and metabolic tumor volume.<sup>34</sup> The previously reported tumor SUV<sub>max</sub> varies substantially, ranging

from an  $SUV_{max}$  cut-off of 9.0 for non-small cell lung cancer to a cut-off of 13.7 for neuroendocrine tumors. The  $SUV_{max}$  cut-off value of cervical cancer, however, remains uncertain, with studies showing this value to be closely related to tumor size, differentiation, and morphology.<sup>35</sup>

In the present study, the  $SUV_{max}$  and  $SUV_{mean}$  of primary cervical cancer lesions detected via PET/MRI were  $23.7 \pm 8.1$  and  $14.2 \pm 4.6$ , respectively, and were significantly higher than those obtained through PET/CT imaging ( $p < 0.001$ ). Interestingly, the difference in the  $SUV_{max}$  and  $SUV_{mean}$  for adjacent organ involvement and/or metastatic lymph nodes was not significantly different between PET/MRI and PET/CT in these patients. From our clinical practice experience, the SUV is considered a half-quantitative index, so its accurate calculation is helpful to determine the range of lesions and metastases.

This retrospective study has three main limitations. The first limitation is the difference in the FDG uptake periods between PET/CT and PET/MRI, which may have affected the PET diagnostic performance and SUVs. The second limitation is that the diagnostic performance for lymph node size was not analyzed. Third, from a technical viewpoint, PET/MRI is still unable to achieve fast scanning of multiple MRI sequences and PET fusion. Therefore, we should constantly optimize MRI sequences for patients with cervical cancer and improve the level of diagnosis.

In summary, PET/MRI is a more efficacious approach to the diagnosis of cervical cancer relative to other available imaging modalities. Primary lesions that are 4 cm in diameter are the diagnostic basis for locally advanced cervical cancer,<sup>36</sup> in addition to serving as the reference basis for cavity radiation therapy. Primary lesions ranging from 2 to 4 cm in size are optimal candidates for preoperative neoadjuvant chemotherapy. Although oncologists can generally evaluate

these tumors through specialized examinations, PET/MRI scans represent a more reliable approach to evaluating these tumors. A meta-analysis conducted by Nie et al.<sup>37</sup> showed that PET/MRI is an extremely sensitive and specific approach to the diagnosis of gynecological pelvic tumors.

It is important to use some degree of caution when interpreting these imaging results, however, because neither PET/MRI nor PET/CT perform as reliably in diagnostic contexts as the gold standard approach of direct pathological examination. The SUVs used in these imaging approaches are not objective and are dependent upon the subjective interpretations of those reviewing the resultant scan data.<sup>38</sup> Despite the overall promise of this technology, there are still many limitations to the PET/MRI modality, necessitating future research and development to improve overall diagnostic reliability. Most importantly, further work is required to optimally integrate PET and MRI technologies, reduce overall operative costs, and improve inter-rater reliability.


### Declaration of conflicting interest

The authors declare that there is no conflict of interest.

### Funding

This research received no specific grant from any funding agency in the public, commercial, or not-for-profit sectors.

### ORCID iD

Jing Gong  <https://orcid.org/0000-0002-8814-736X>

### References

1. Ferlay J, Soerjomataram I, Dikshit R, et al. Cancer incidence and mortality worldwide: sources, methods and major patterns in GLOBOCAN 2012. *Int J Cancer* 2015; 136: E359–E386.

2. Stehman FB, Bundy BN, DiSaia PJ, et al. Carcinoma of the cervix treated with radiation therapy. I. A multi-variate analysis of prognostic variables in the Gynecologic Oncology Group. *Cancer* 1991; 67: 2776–2785.
3. Castellani F, Nganga EC, Dumas L, et al. Imaging in the pre-operative staging of ovarian cancer. *Abdom Radiol (NY)* 2019; 44: 685–696.
4. Eifel PJ, Morris M, Wharton JT, et al. The influence of tumor size and morphology on the outcome of patients with FIGO stage IB squamous cell carcinoma of the uterine cervix. *Int J Radiat Oncol Biol Phys* 1994; 29: 9–16.
5. Garipagaoglu M, Tulunay G, Kose MF, et al. Prognostic factors in stage IB-IIA cervical carcinomas treated with postoperative radiotherapy. *Eur J Gynaecol Oncol* 1999; 20: 131–135.
6. Lagasse LD, Creasman WT, Shingleton HM, et al. Results and complications of operative staging in cervical cancer: experience of the Gynecologic Oncology Group. *Gynecol Oncol* 1980; 9: 90–98.
7. Soutter WP, Hanoch J, D'Arcy T, et al. Pretreatment tumour volume measurement on high-resolution magnetic resonance imaging as a predictor of survival in cervical cancer. *BJOG* 2004; 111: 741–747.
8. Grigsby PW, Siegel BA and Dehdashti F. Lymph node staging by positron emission tomography in patients with carcinoma of the cervix. *J Clin Oncol* 2001; 19: 3745–3749.
9. Hany TF, Steinert HC, Goerres GW, et al. PET diagnostic accuracy: improvement with in-line PET-CT system: initial results. *Radiology* 2002; 225: 575–581.
10. Capitano S, Nordin AJ, Noraini AR, et al. PET/CT in nononcological lung diseases: current applications and future perspectives. *Eur Respir Rev* 2016; 25: 247–258.
11. Seemann MD. Whole-body PET/MRI: the future in oncological imaging. *Technol Cancer Res Treat* 2005; 4: 577–582.
12. Von Schulthess GK and Schlemmer HP. A look ahead: PET/MR versus PET/CT. *Eur J Nucl Med Mol Imaging* 2009; 36: S3–S9.
13. Herzog H. PET/MRI: challenges, solutions and perspectives. *Z Med Phys* 2012; 22: 281–298.
14. Yoon HS, Ko GB, Kwon SI, et al. Initial results of simultaneous PET/MRI experiments with an MRI-compatible silicon photomultiplier PET scanner. *J Nucl Med* 2012; 53: 608–614.
15. Stecco A, Buemi F, Cassarà A, et al. Comparison of retrospective PET and MRI-DWI (PET/MRI-DWI) image fusion with PET/CT and MRI-DWI in detection of cervical and endometrial cancer lymph node metastases. *Radiol Med* 2016; 121: 537–545.
16. Zaidi H, Montandon ML and Slosman DO. Magnetic resonance imaging-guided attenuation and scatter corrections in three-dimensional brain positron emission tomography. *Med Phys* 2003; 30: 937–948.
17. Hofmann M, Bezrukov I, Mantlik F, et al. MRI-based attenuation correction for whole-body PET/MRI: quantitative evaluation of segmentation- and atlas-based methods. *J Nucl Med* 2011; 52: 1392–1399.
18. Boss A, Stegger L, Bisdas S, et al. Feasibility of simultaneous PET/MR imaging in the head and upper neck area. *Eur Radiol* 2011; 21: 1439–1446.
19. Drzezga A, Souvatzoglou M, Eiber M, et al. First clinical experience with integrated whole-body PET/MR: comparison to PET/CT in patients with oncologic diagnoses. *J Nucl Med* 2012; 53: 845–855.
20. Platzek I, Beuthien-Baumann B, Schneider M, et al. PET/MRI in head and neck cancer: initial experience. *Eur J Nucl Med Mol Imaging* 2013; 40: 6–11.
21. Heusch P, Buchbender C, Beiderwellen K, et al. Standardized uptake values for [<sup>18</sup>F] FDG in normal organ tissues: comparison of whole-body PET/CT and PET/MRI. *Eur J Radiol* 2013; 82: 870–876.
22. Botsikas D, Kalovidouri A, Becker M, et al. Clinical utility of 18F-FDG-PET/MR for preoperative breast cancer staging. *Eur Radiol* 2016; 26: 2297–2307.
23. Surov A, Meyer HJ, Schob S, et al. Parameters of simultaneous 18F-FDG-PET/MRI predict tumor stage and several histopathological features in uterine cervical cancer. *Oncotarget* 2017; 8: 28285–28296.
24. King AD, Ma BB, Yau YY, et al. The impact of 18F-FDG PET/CT on assessment

- of nasopharyngeal carcinoma at diagnosis. *Br J Radiol* 2008; 81: 291–298.
25. Choi J, Kim HJ, Jeong YH, et al. The role of (18)F-FDG PET/CT in assessing therapy response in cervix cancer after concurrent chemoradiation therapy. *Nucl Med Mol Imaging* 2014; 48: 130–136.
  26. Tsukamoto N, Kojima M, Hasegawa M, et al. The usefulness of (18)F-fluorodeoxyglucose positron emission tomography ((18)F-FDG-PET) and a comparison of (18)F-FDG-pet with (67)gallium scintigraphy in the evaluation of lymphoma: relation to histologic subtypes based on the World Health Organization classification. *Cancer* 2007; 110: 652–659.
  27. Carril M. Activatable probes for diagnosis and biomarker detection by MRI. *J Mater Chem B* 2017; 5: 4332–4347.
  28. Shao K, Singha S, Clemente-Casares X, et al. Nanoparticle-based immunotherapy for cancer. *ACS Nano* 2015; 9: 16–30.
  29. Sawicki LM, Kirchner J, Grueneisen J, et al. Comparison of (18)F-FDG PET/MRI and MRI alone for whole-body staging and potential impact on therapeutic management of women with suspected recurrent pelvic cancer: a follow-up study. *Eur J Nucl Med Mol Imaging* 2018; 45: 622–629.
  30. Bollineni VR, Ytre-Hauge S, Bollineni-Balabay O, et al. High diagnostic value of 18F-FDG PET/CT in endometrial cancer: systematic review and meta-analysis of the literature. *J Nucl Med* 2016; 57: 879–885.
  31. Kim HS, Kim CK, Park BK, et al. Evaluation of therapeutic response to concurrent chemoradiotherapy in patients with cervical cancer using diffusion-weighted MR imaging. *J Magn Reson Imaging* 2013; 37: 187–193.
  32. Kim SK, Choi HJ, Park SY, et al. Additional value of MR/PET fusion compared with PET/CT in the detection of lymph node metastases in cervical cancer patients. *Eur J Cancer* 2009; 45: 2103–2109.
  33. Grueneisen J, Schaarschmidt BM, Heubner M, et al. Implementation of FAST-PET/MRI for whole-body staging of female patients with recurrent pelvic malignancies: a comparison to PET/CT. *Eur J Radiol* 2015; 84: 2097–2102.
  34. Schwarz JK, Siegel BA, Dehdashti F, et al. Association of posttherapy positron emission tomography with tumor response and survival in cervical carcinoma. *JAMA* 2007; 298: 2289–2295.
  35. Xin J, Ma Q, Guo Q, et al. PET/MRI with diagnostic MR sequences vs PET/CT in the detection of abdominal and pelvic cancer. *Eur J Radiol* 2016; 85: 751–759.
  36. Small W Jr, Bacon MA, Bajaj A, et al. Cervical cancer: a global health crisis. *Cancer* 2017; 123: 2404–2412.
  37. Nie J, Zhang J, Gao J, et al. Diagnostic role of 18F-FDG PET/MRI in patients with gynecological malignancies of the pelvis: a systematic review and meta-analysis. *PLoS One* 2017; 12: e0175401.
  38. Bernstine H, Domachevsky L, Nidam M, et al. 18F-FDG PET/MR imaging of lymphoma nodal target lesions: comparison of PET standardized uptake value (SUV) with MR apparent diffusion coefficient (ADC). *Medicine (Baltimore)* 2018; 97: e0490.